

Wide magnetic field range of Ni-P/PZT/Ni-P cylindrical layered magnetoelectric composites

D. A. Pan,^{1,a)} J. Wang,¹ Z. J. Zuo,¹ S. G. Zhang,¹ L. J. Qiao,¹ and A. A. Volinsky²

¹*Institute of Advanced Materials and Technology, University of Science and Technology Beijing, Beijing 100083, China*

²*Department of Mechanical Engineering, University of South Florida, Tampa, Florida 33620, USA*

(Received 21 January 2014; accepted 28 February 2014; published online 25 March 2014)

The Ni-P/PZT/Ni-P cylindrical layered magnetoelectric (ME) composites were prepared by electroless deposition. The Ni-P layer has an amorphous nanocrystalline structure. The ME effect in the axial mode of the Ni-P/PZT/Ni-P cylindrical layered composites is similar to that of Ni/PZT/Ni. The Ni-P/PZT/Ni-P composite has lower bias magnetic field of 120 Oe to induce a maximum $\alpha_{E,A}$ and 0.5 kOe to generate $\alpha_{E,A}$ linear increase at the resonance frequency, which may be related to the high permeability of the Ni-P layer. This discovery contributes to the ME devices miniaturization and expands the magnetic field detection range at both low and high magnetic fields. © 2014 AIP Publishing LLC. [<http://dx.doi.org/10.1063/1.4868415>]

The magnetoelectric (ME) effect is characterized by an electric polarization induced by an applied magnetic field, or conversely, a magnetization induced by an applied electric field.¹ Multiple potential applications, such as sensors, actuators, and transducers, have been proposed for the ME materials, based on their unique multifunctionality.^{2,3} Compared with homogeneous ME composites, layered ME composites exhibit much higher ME voltage coefficient due to the combination of magnetostrictive and piezoelectric effects.⁴

Currently, there are multiple methods available for preparing layered ME composites with different kinds of interfacial bonding, including bonding with epoxy,⁵ electrodeposition,^{6,7} and electroless deposition.^{8,9} The objective and the development trend of magnetoelectric devices are to obtain giant magnetoelectric properties under low bias magnetic field to meet the integrated design needs. It has been reported that lowering the required bias magnetic field (H_{DC}) by the use of an alternative magnetostrictive phase would enable miniaturization of laminated ME devices for magnetic sensing and transducer applications.¹⁰ Zhai *et al.*¹¹ have prepared ME laminates with high magnetic permeability, based on the Metglas layers laminated together with polyvinylidene-fluoride (PVDF) piezopolymer layers, which showed giant ME voltages under low bias magnetic field.

Typical characteristics of some representative layered ME sensors are given in Table I. Comparing the advantages and disadvantages, it is therefore valid to consider that electroless deposition is a convenient method to obtain functional films with good interfacial bonding.¹² Nickel is a kind of conventional magnetic material suitable as the piezomagnetic component in the ME composites. Addition of the light elements (H, B, N, and P) to Ni can effectively form amorphous nanocrystalline structures, which exhibit enhanced magnetic properties, such as high magnetic induction, high permeability, and low loss.^{13,14} In addition, it is convenient

to attain Ni-P nano-alloy films by electroless deposition.^{15,16} In view of the above, Ni-P/PZT/Ni-P cylindrical layered ME composites have been prepared by the electroless deposition. The typical curve of the ME voltage coefficient, $\alpha_{E,A}$, dependence on the DC bias magnetic field, H_{DC} , shifts to the left, towards lower H_{DC} values at the resonance frequency, compared with previously reported cylindrical ME composites.

The preparation of the Ni-P/PZT/Ni-P cylindrical layered composites is described next. The PZT cylinders with the $\Phi 20 \times \Phi 18 \times 10$ mm³ dimensions were polarized in an electrical field applied along the radial direction after electroplating a thin Ni layer on its outer surface. The samples were pretreated with supersonic cleaning and sulfuric acid cathodic activation processes prior to the electroless deposition. The electroless bath composition and the deposition conditions are shown in Table II. The ME effect of the Ni-P/PZT/Ni-P cylindrical layered composites was measured in the ME measurement system, where both constant (H_{DC}) and alternating (δH) magnetic fields were applied parallel (axial mode) to the cylinder height (axis) direction.⁴ The ME voltage coefficient was calculated as $\alpha_E = \delta V / (t_{PZT} \delta H)$, where t_{PZT} is the PZT layer thickness and δH is the amplitude of the AC magnetic field generated by the Helmholtz coils. The AC current flowing through the coil with the applied magnetic field amplitude of $\delta H = 1.2$ Oe was equal to 1 A.

The resulting total thickness of the inside and the outside Ni-P layers was approximately 400 μ m. The schematic of the Ni-P/PZT/Ni-P cylindrical layered composite is shown in Fig. 1(a). Fig. 1(b) is the scanning electron microscopy (SEM) image of the interface between the electroless deposited Ni-P layer and the PZT layer, showing adequate mechanical coupling between the two phases.

As seen in the SEM micrograph in Fig. 2(a), the electroless deposited Ni-P layer is dense and smooth. The energy dispersive X-ray spectrum (EDX) in Fig. 2(b) indicates that there are both Ni and P elements in the electroless deposited layer, in which phosphorus content is approximately 9.8 wt. % with no impurities present. The X-ray diffraction (XRD) pattern of the Ni-P layer is shown in Fig. 2(c). The

^{a)}Author to whom correspondence should be addressed. Electronic mail: pandean@mater.usfb.edu.cn

TABLE I. Typical characteristics of some representative layered ME sensors.

Representative layered ME sensors	Advantages	Disadvantages
Terfenol-D/PZT bonding with epoxy	Large ME voltage coefficient (~ 10 V/cm·Oe at the resonance frequency with $H_{DC} \approx 1.3$ kOe ¹⁷)	(1) High dc magnetic bias H_{DC} is required to obtain maximum ME voltage coefficients. ³ (2) Bonding layer induces non-rigid contact, fatigue, and aging effects. ⁸
Transition metal element Ni/PZT prepared by electrodeposition	Rigid contact between the magnetostrictive and piezoelectric phases ^{6,7}	(1) Electrodes cause negative effects to reduce the ME coupling. ⁴ (2) Unable to get small nanocrystals or nano amorphous.
Metglas/PVDF bonding with epoxy	Giant ME voltage coefficient caused by very low dc magnetic bias (~ 7.2 V/cm·Oe at 1 kHz with $H_{DC} \approx 8$ Oe ¹¹)	(1) Complex and difficult to prepare. (2) Same disadvantage as (2) for Terfenol-D/PZT.

TABLE II. Electroless bath composition and deposition conditions.

Chemical composition	Concentration	Conditions
NiSO ₄ ·6H ₂ O	27 g/l	pH = 4.7
NaH ₂ PO ₂ ·H ₂ O	30 g/l	$T = 85^\circ\text{C}$
Na ₃ C ₆ H ₅ O ₇ ·2H ₂ O	20 g/l	Deposition rate = 20 $\mu\text{m/h}$
NaAC	5 g/l	
Sodium lauryl sulfate	0.4 g/l	
Stabilizer	1 mg/l	

diffuse diffraction peak around $2\theta = 45^\circ$ indicates that the Ni-P layer has amorphous structure.¹⁸

The behavior of the magnetoelectric voltage coefficient, $\alpha_{E,A}$, with the DC bias magnetic field H_{DC} and frequency f is consistent with that of the Ni/PZT/Ni cylindrical composites.⁴ Fig. 3(a) shows the frequency dependence of $\alpha_{E,A}$ at $H_{DC} = 120$ Oe, where a sharp resonance peak appears at 59.7 kHz. The enhanced ME coefficient of 1 V/cm·Oe is related to the electromechanical resonance.¹⁹ Fig. 3(b) shows the $\alpha_{E,A}$ dependence on H_{DC} at the resonance frequency of $f = 59.7$ kHz. The $\alpha_{E,A}$ is increasing with H_{DC} until the local maximum value of 1 V/cm·Oe is reached at 120 Oe ($H_m = 120$ Oe). Then the $\alpha_{E,A}$ increases linearly with H_{DC} between 0.5 kOe and 5 kOe ($R = 0.9996$).

Bi *et al.*⁴ have prepared Ni/PZT/Ni cylindrical layered composites by electroless deposition, with the local maximum ME voltage coefficient at $H_m = 270$ Oe and the linear region starting at $H_{DC,i} = 1.5$ kOe for the H_{DC} dependence of $\alpha_{E,A}$ at the resonance frequency. Compared with the two composites, the results show that the curve of $\alpha_{E,A}$ dependence on H_{DC}

integrally shifts to the left at the resonance frequency, and H_m and $H_{DC,i}$ shift of 150 Oe and 1 kOe, respectively. It is an outstanding advantage of these composites over other previously reported types, offering potential in practical applications that not only reduces the size of the magnetoelectric sensors at the low magnetic field, but also expands the detection scope of magnetic field detectors at the high magnetic field. For this phenomenon in Fig. 3(b), the possible reason is the amorphous nanocrystalline structure of the Ni-P layer, resulting in high permeability of the magnetostrictive layer affecting the $\alpha_{E,A}$ behavior.

Amorphous nanocrystalline Ni-P layers have no long range periodic crystal structure (only short-range order), and also no macroscopic magnetocrystalline anisotropy energy, which means that they are easily magnetized in all directions. It is reported that for amorphous Ni-P layers, the saturation magnetization (M_s) is 1.198 emu/g, the residual magnetization (M_r) is 0.205 emu/g, the coercive force (H_c) is 304.34 Oe, and the rectangularity ratio of the hysteresis loop (M_r/M_s) is less than 0.2.²⁰ Hence, Ni-P layers have the high permeability ($\propto 1/M_r/M_s$) and act to powerfully concentrate external flux into the laminate, resulting in stronger magnetic induction \mathbf{B} ($= \mu_0 \mu_r H$), in turn resulting in higher effective piezomagnetic coefficient.²¹ The stronger piezoinductive effect between the Ni-P layer and the PZT cylinder produces significant changes in the $\alpha_{E,A}$ of the Ni-P/PZT/Ni-P cylindrical layered composites.²²

Zhai¹¹ *et al.* have attained Metglas/polyvinylidene-fluoride ME laminates, which achieved a maximum ME coefficient with an applied magnetic bias of only $H_{DC} = 8$ Oe. The Metglas is a kind of amorphous alloy with high magnetic

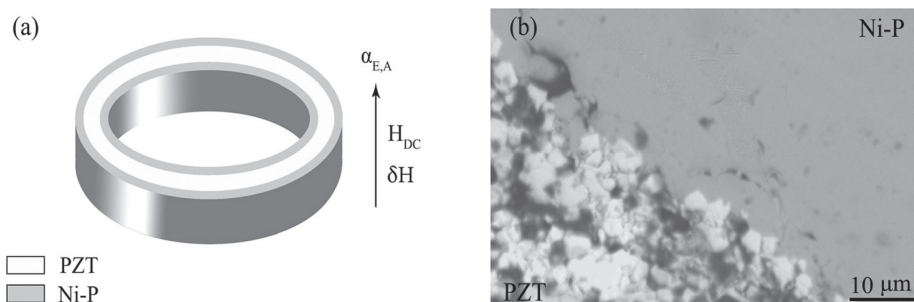


FIG. 1. (a) Ni-P/PZT/Ni-P cylindrical layered composite schematics; (b) Cross-sectional SEM micrograph of the Ni-P/PZT interface.

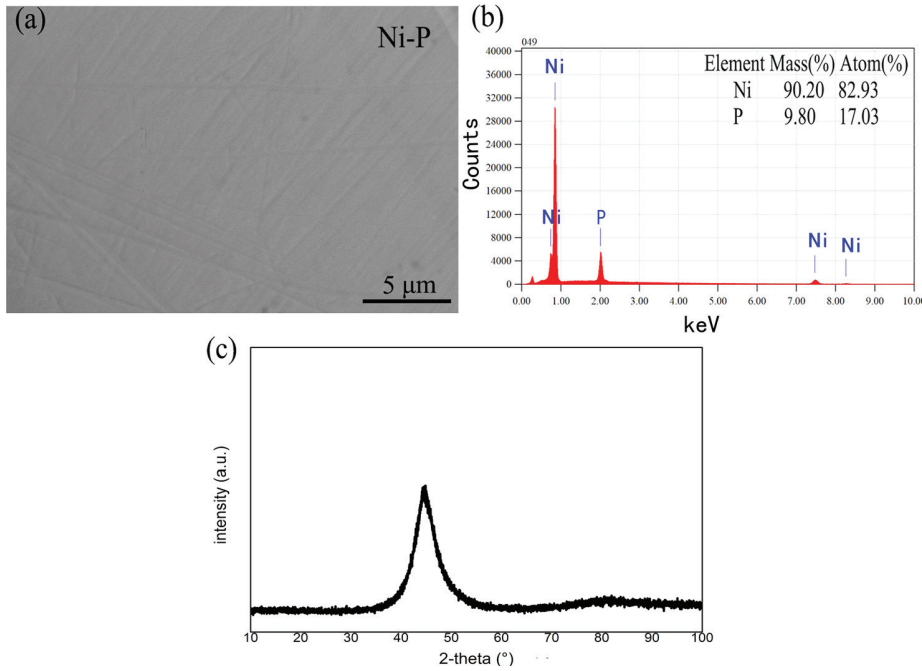


FIG. 2. (a) Cross-sectional SEM micrograph of the electroless deposited Ni-P layer. (b) EDX spectrum of the Ni-P layer. (c) XRD pattern of the Ni-P layer.

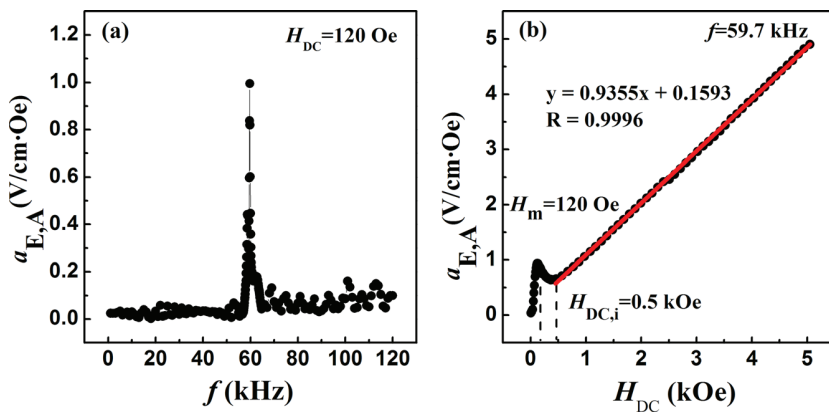


FIG. 3. (a) Ac magnetic field frequency f dependence of $\alpha_{E,A}$ with $H_{DC} = 120$ Oe, (b) the H_{DC} dependence of $\alpha_{E,A}$ at the resonance frequency of $f = 59.7$ kHz, and the straight line shows the linear fitting of $\alpha_{E,A}$ dependence on H_{DC} from 0.5 kOe to 5 kOe.

permeability. Likewise, phosphorus content of 9.8% in the Ni-P layer causes a mixed state of amorphous and microcrystalline structure; however, the Ni-P layer can have completely amorphous structure by adjusting the phosphorus content. Correspondingly, the required H_m and $H_{DC,i}$ can be further decreased, and it can be speculated that there will be further left shift with the phosphorus content increase. In the future experiments, the effects of phosphorus content on magnetoelectric properties will be studied in detail.

In conclusion, at the resonance frequency, the curve of the ME voltage coefficient, $\alpha_{E,A}$, dependence on the DC bias magnetic field, H_{DC} , in the Ni-P/PZT/Ni-P cylindrical layered ME composites presents a maximum at $H_m = 270$ Oe and the linear relationship above $H_{DC,i} = 1.5$ kOe, indicating a notable left shift in contrast to other ME cylindrical laminates. The high $\alpha_{E,A}$ can be caused by the high permeability of the Ni-P layer owing to its amorphous structure. These composites have good potential applications at both low and high magnetic fields.

This work was supported by the National Natural Science Foundation of China (Nos. 51004011, 51174247, 51002141, and U1360202), by Research Fund for the Doctoral Program

of Higher Education (No. 2010000612003), by the Fundamental Research Funds for the Central Universities (No. FRF-TP-12-151A), by the National Key Technology R&D Program (Nos. 2012BAC02B01 and 2012BAC12B05), and by the National High-Tech Research and Development Program of China (No. 2012AA063202).

¹L. D. Landau and J. B. Sykes, *Electrodynamics of Continuous Media* (Pergamon press Oxford, 1960).

²W. Wu, K. Bi, and Y. G. Wang, *J. Mater. Sci.* **46**, 1602 (2011).

³C. Nan, M. I. Bichurin, S. Dong, D. Viehland, and G. Srinivasan, *J. Appl. Phys.* **103**, 031101 (2008).

⁴K. Bi, W. Wu, Q. L. Gu, H. N. Cui, and Y. G. Wang, *J. Alloy Compd.* **509**, 5163 (2011).

⁵J. Ryu, A. V. Carazo, K. Uchino, and H. Kim, *Jpn. J. Appl. Phys., Part 1* **40**, 4948 (2001).

⁶D. A. Pan, Y. Bai, W. Y. Chu, and L. J. Qiao, *Smart Mater. Struct.* **16**, 2501 (2007).

⁷D. A. Pan, Y. Bai, W. Y. Chu, and L. J. Qiao, *J. Phys.: Condens. Matter* **20**, 025203 (2008).

⁸W. Wu, Y. G. Wang, and K. Bi, *J. Magn. Magn. Mater.* **323**, 422 (2011).

⁹C. Nan, G. Liu, and Y. Lin, *Appl. Phys. Lett.* **83**, 4366 (2003).

¹⁰J. Zhai, Z. Xing, S. Dong, J. Li, and D. Viehland, *Appl. Phys. Lett.* **88**, 062510 (2006).

¹¹J. Zhai, S. Dong, Z. Xing, J. Li, and D. Viehland, *Appl. Phys. Lett.* **89**, 083507 (2006).

¹²K. Bi and Y. G. Wang, *Solid State Commun.* **150**, 248 (2010).

- ¹³J. Petzold, *J. Magn. Magn. Mater.* **242**, 84 (2002).
- ¹⁴J. Petzold, *Scr. Mater.* **48**, 895 (2003).
- ¹⁵S. Ge, Z. Wu, M. Zhang, W. Li, and K. Tao, *Ind. Eng. Chem. Res.* **45**, 2229 (2006).
- ¹⁶Z. J. Zhang and Y. Wang, *Mater. Rev.* **20**, 342 (2006).
- ¹⁷Z. J. Zuo, D. A. Pan, Y. M. Jia, S. G. Zhang, and L. J. Qiao, *AIP Adv.* **3**, 122114 (2013).
- ¹⁸X. S. Li, J. B. Wang, and L. H. Du, *Electroplat. Pollut. Control* **27**, 20 (2007).
- ¹⁹D. A. Pan, Y. Bai, W. Y. Chu, and L. J. Qiao, *J. Phys. D: Appl. Phys.* **41**, 022002 (2008).
- ²⁰D. L. Zhao, Z. M. Lu, and Z. M. Shen, *Acta Mater. Compositae Sin.* **21**, 54 (2004).
- ²¹S. Dong, J. Zhai, J. Li, and D. Viehland, *Appl. Phys. Lett.* **89**, 122903 (2006).
- ²²Y. K. Fetisov, D. V. Chashin, and G. Srinivasan, *J. Appl. Phys.* **106**, 044103 (2009).